Control of a Hydraulic Regenerative Braking System for a Heavy Goods Vehicle

W. J. B. Midgley and D. Cebon[1]
Department of Engineering,
University of Cambridge,
CB2 1PZ UK

Submitted to IMech E, Part D, J. Auto. Eng., December 2014
Response to reviewers 30 June, 2015

Summary

This paper investigates the fuel consumption of an articulated vehicle with a hydraulic regenerative braking system. The vehicle is a 4-axle tractor-semitrailer with volume-limited payload. It is equipped with hub-mounted hydraulic pump-motor units that pump fluid from a low-pressure reservoir to a high-pressure reservoir during braking events and generate a propulsive torque when high pressure fluid flows through them to the low pressure reservoir during acceleration.

Several possible control strategies are proposed and simulated using a validated mathematical model of the fuel consumption of the vehicle. A global optimization calculation indicates that the maximum possible reduction in fuel consumption due to the regenerative braking system is 11-22%, depending on the drive cycle. The simulations indicate that the simple 'greedy' algorithm would decrease fuel consumption by 9-17% for the same conditions. Two heuristic algorithms and a Model-Predictive-Control approach were also investigated. Although these more sophisticated controllers were able to improve on the 'greedy' algorithm slightly for some conditions, they may not be implementable in practice.

1 Introduction

Previous research has shown that adding regenerative braking to a heavy goods vehicle (HGV) can reduce the vehicle's energy usage by up to 30% for urban drive cycles [1-5]. It has also been shown that hydraulic energy storage and actuation systems are the lightest and smallest for this purpose [6]. There is no consensus in the literature regarding the best control strategy for hydraulic regenerative braking. The 'greedy' control approach (so-named because it attempts to harvest (and use) energy at every opportunity) is simple and effective [7], but it is thought that more sophisticated control strategies could improve the benefits.

There are many papers concerned with energy saving strategies for electric hybrid vehicles. These tend to focus on the state of charge (SOC) of the battery, and try to reduce the amount of fuel used by the vehicle, without taking the battery outside of pre-determined SOC limits [8].

[1] Corresponding author: dc@eng.cam.ac.uk, University Engineering Department, Trumpington St, Cambridge, CB2 1PZ, UK.

There are several different algorithms used for this optimisation, including: neural network control [9]; combined sliding mode and neural network control [10]; and driving pattern recognition [11, 12]. The most effective of these require intensive calculations and are difficult to execute in real-time [13-15]. Studies by Lin et al. [3, 8, 11, 12, 14] on parallel hybrid electric trucks have concluded that a 28% increase in fuel economy is possible for a simple stop-start cycle. These results come from intricate vehicle simulation models, paired with sophisticated feed-forward control and dynamic programming.

However, optimal control of hydraulic regenerative braking on an HGV is more complicated than these electric hybrid cases, for three main reasons:

1. The non-linear effect of inefficiencies in the hydraulic pump/motors. These inefficiencies depend on both the speed and the pressure difference across each of the pump/motors;
2. For the light, small fixed-displacement hydraulic pump/motors investigated in this study, there is no fine-grained control of torque; they are either on and providing full torque, or idling and not providing any torque;
3. The non-linear effects of the driver model, and the engine efficiency map.

The aim of this research is therefore to investigate possibilities for optimising the control of the hydraulic regenerative braking system, with the goal of finding a strategy that can be implemented in real-time.

2 Mathematical Model

2.1 Vehicle Model

The vehicle used for this investigation was a 4x2 tractor unit pulling a two-axle, 13.5m long, semitrailer with a maximum gross vehicle weight of 33 tonnes (see Figure 1 and Table 1). Such vehicles are often used for urban delivery of volume-limited freight in the UK. This vehicle duty is ideally suited to regenerative braking [7].

The mathematical model of the vehicle's fuel consumption used in the study was the same as the validated tractor semi-trailer model described by Midgley et al [16]. A schematic, top-level overview of this model is provided in Figure 2. It includes the interaction of the driver model (taken from [17]) with the vehicle, through the throttle demand, gear changes and brake demand, to regulate the speed and acceleration of the vehicle. More detail about the vehicle model can be found in [16, 18].

The engine map, aerodynamic drag and rolling resistance parameters were measured in full scale tests on an experimental vehicle [17]. Experimental validation of the original tractor semi-trailer model is provided in [17]. A representative result from this paper is given in Figure 3, which shows that the fuel consumption of the model and the test vehicle agree well over a two-minute acceleration to the vehicle's maximum speed.

2.2 Hydraulic Regenerative Braking System

The hydraulic regenerative braking system was assumed to act on the two axles of a semi-trailer, as shown in Figure 1. Given the lack of space on modern European tractor units, it was seen as infeasible to place regenerative braking on the drive axles of the tractor unit.

A schematic of the hydraulic system is given in Figure 4, showing the high- and low-pressure (HP and LP) accumulators, a 3-position valve, and two fixed-displacement hydraulic pump/motors (PMs).

In deceleration mode, the valve is shifted so that as the wheels turn, the PMs drive fluid from the LP accumulator to the HP accumulator, and a negative (braking) torque is generated. In freewheel mode, the valve is centred, and the PMs are disengaged, removing parasitic losses. In acceleration mode, fluid is routed through the motors from the HP accumulator to the LP accumulator, producing a positive (driving) torque. More detail about the hydraulic regenerative braking system can be found in [7].

The regenerative braking system was assumed to be installed on the vehicle in such a way that it did not interfere with the payload volume of the vehicle. By installing the accumulators and associated valves under the deck of the trailer, between the hitch point and the wheels, no storage space would be sacrificed to the system (see Figure 4). However, the additional weight of the system was taken into account, because it affects the rolling resistance and energy flows during acceleration and deceleration. It was assumed to be 230kg, based on data available in the public domain for the weights of carbon-fibre accumulators [19] and the PMs [20]. From the numbers in Table 1 it can be seen that this 230kg represents an increase in the gross vehicle weight of 1%, resulting in a similar 1% increase in the rolling resistance force generated by the tyres.

The acceleration and deceleration demands were also fed to the regenerative braking system, so that it could make decisions on whether to produce additional braking/accelerating torque.

The hydraulic pump/motors (PMs) can be in one of three states: off and freewheeling; on and providing positive torque to the vehicle (acceleration); and providing negative torque to the vehicle (braking) (see Figure 4). The PMs are controlled in pairs (front left/right and rear left/right), and the control command to each of the pairs is updated once per second (1Hz). The reasonably low update rate is due to the response time of the system – any shorter and the system could be switched on and off before the PMs had a chance to respond. The supervisory controller operates at a higher frequency (100Hz) to ensure that the system does not overpressure the hydraulic accumulators, or overspeed the hydraulic PMs. The characteristics of the PMs were modelled using performance maps provided by the manufacturer [20]. Hydraulic losses were assumed to be proportional to the flowrate according to:

$$\Delta P = \frac{1}{2} k \rho v_f^2 \tag{1}$$

where ΔP is the pressure drop across a piece of pipe, k is the hydraulic loss coefficient, and v_f is the velocity of the fluid through the pipe. Values for k were taken from Merritt [21].

This combined regenerative braking computer model was run over predominantly urban drive cycles to obtain the fuel usage of the vehicle under various control scenarios. As in previous papers [1, 16, 18], an energy index based on the volume of freight carried by the vehicle (with units of kJ/[m^3.km], abbreviation: EI_v) was used for comparing the fuel usage of the control scenarios.

$$EI_V = \frac{\text{Fuel Energy Used}}{\text{Payload Volume} \times \text{Distance Covered}} \quad (2)$$

This measure takes into account the added mass of the hydraulic system (which increases the rolling resistance loss), as discussed in [16, 18].

The control problem is to choose the times at which the pump/motor units should be switched between control modes so as to minimise the fuel consumption of the vehicle for a given drive cycle.

2.3 'Greedy' Algorithm

The 'greedy' algorithm is simple to implement when decelerating, store as much energy as possible as soon as it is available; when accelerating use any stored energy if possible [22]. During braking, as much of the torque demand as possible is generated by the regenerative braking system, and any shortfall in torque is demanded from the 'foundation' brakes. Acceleration is similar in that as much of the torque demand as possible is met by the regenerative braking, and any remaining torque is demanded from the vehicle's engine. The amount of braking force demanded from each axle is proportional to that axle's normal (i.e. weight) force, further details about this are available in [7].

This approach does not require any foreknowledge of the drive cycle, terrain, or other conditions ahead. In this project, greedy was seen as the baseline performance against which other controllers would be compared. (The optimised results prove the upper bound for performance and therefore fuel saving.)

3 Controller Development

Due to the unusual nature of this control problem (highly non-linear, multi-input-multi-output, unique hybrid configuration), it was unclear what the lower bound of the energy index (EI_v) was for a given drive cycle. The lower bound was therefore obtained by running several global optimisers over one drive cycle, minimising the EI_v for this cycle, and choosing the optimiser that returned the best EI_v for the cycle. This was necessary because each global optimiser converged to slightly different local minima and it was not possible to establish whether the global minimum was reached or not.

3.1 Lower Bound through Global Optimisation

There are several different methods for performing 'global' optimisation, though most of them operate in a similar manner: Given a function to minimise and an initial start point, the algorithm generates a new set of function inputs and then evaluates the function at these points. It then repeats this process until a stopping constraint is violated or the function converges to a minimum. It is often not possible to establish whether this minimum is the true global minimum or not.

In the application investigated here, the input parameters were the switching on and off times sampled every one second through the drive cycle. The optimisation process sought to find the set of switching times that minimised the total energy consumption over the given drive cycle.

The three global optimisation routines that were thought applicable to this problem were 'pattern search' [23], 'simulated annealing' [24] and a 'genetic algorithm' [25]. The main difference between these is the way that the new set of input points is generated.

Each of these three algorithms was given the same problem to solve, with the same constraints (where possible), the same starting point, and similar tolerances for stopping criteria. The results of this comparison are shown in Figure 5, where each global optimisation technique is compared to the results of the 'greedy' algorithm. This shows that large improvements can be made over the greedy strategy for the UDDS [26] and the NYC [26] cycles (up to 10%), but only small gains are possible on the HHDDT-T [27] and NEDC [28] cycles (1% or 2%). Pattern search gave the best results in each case, and the genetic algorithm came second. It should be stressed that none of these optimization algorithms could be implemented as a real-time controller, because each was able to repeatedly alter the switching settings backwards and forwards over each drive cycle until it reached a minimum. Clearly this would not be possible in real-time control.

3.2 Controllers

A greedy strategy is very rarely the optimal strategy [29], and is therefore not always used in the control of existing hydraulic hybrids [30]. After establishing the upper bound on EI_v reduction by optimisation, the intention was to develop other control strategies that could approach these improved levels of fuel saving, and to compare these strategies to the greedy strategy. Three different approaches were tested. These were named: 'power consumption heuristic', 'fuel consumption heuristic' and 'model predictive control (MPC)'.

Some heuristic strategies require full and perfect knowledge of the future conditions (speed, acceleration, etc.), as well as an accurate model of the vehicle. This is not possible in practice, as a vehicle's route and velocity profile will change dynamically with external factors such as other vehicles on the road, and traffic management systems such as traffic lights and roundabouts. However, the aim of this paper is to compare the results from each of the heuristics over each of the cycles, to determine if there is a common threshold that could be used for any cycle. A secondary aim was to compare results from the heuristics with those from the greedy strategy, to determine whether alternative strategies and additional computational effort could significantly reduce fuel consumption.

3.2.1 'Power Consumption Heuristic' Controller

The system is likely to benefit most from regenerative braking if the positive drive torque is added when the instantaneous power of the vehicle is highest. On level ground, the instantaneous power, $\dot{E}_v$, required to accelerate the vehicle is approximately:

$$\dot{E}_v = \left(m_v a_v + \frac{1}{2}\rho v^2 C_d A + C_r m_v g \right) v_v \tag{3}$$

where m_v is the mass of the vehicle, v_v is the vehicle's speed, a_v is the instantaneous acceleration, ρ is the density of air, C_d is the aerodynamic drag coefficient, A is the frontal area of the vehicle, C_r is the rolling resistance coefficient and g is acceleration due to gravity

(9.81 m/s²). Aerodynamic drag is generally small at the low (urban) speeds when regenerative braking is relevant. Since $C_r g$ is typically up to an order of magnitude less than the longitudinal acceleration a_v during a regenerative braking event, Equation (3) can be simplified to:

$$\dot{E}_v \approx m_v a_v v_v \tag{4}$$

The vehicle was simulated over each of the drive cycles without regenerative braking to derive the instantaneous power profiles of the vehicle for each cycle. A cumulative density function (CDF) [31, 32] of the instantaneous power was then calculated (see Figure 6). For each cycle, a threshold percentile level was chosen by iterating through a range of thresholds (0-100% in 5% steps). The threshold that resulted in the lowest fuel use was chosen (so-called 'brute force'). If the instantaneous power is higher than this value, the system is switched on. During deceleration, the greedy strategy is used, in order to maximise the energy recouped by the regenerative braking system.

There is a further subtlety with this approach. The PMs are only able to switch on below a certain speed, in order to prevent damage to the rotating components in the PM, and so any velocity points above this threshold will skew the CDF. A corrected CDF, using only the parts of the cycle where velocity is below 12.7m/s (the maximum speed of the PMs) is shown in Figure 7. The resulting thresholds used for the four different cycles are given in Table 2.

This approach requires perfect preview of cycle ahead and an accurate model of the vehicle in order to generate the CDF and produce the threshold values for the switching logic. From the results given in Table 3 and Figure 8 it can be seen that this heuristic approach reduces fuel usage by more than the greedy strategy, but not to the level of the global optimiser. This approach requires perfect preview of cycle ahead and an accurate model of the vehicle in order to generate the CDF and produce the threshold values for the switching logic. This may not be possible in practice.

3.2.2 'Fuel Consumption Heuristic' Controller

This heuristic controller provides positive torque from the regenerative braking system when the instantaneous fuel usage of the vehicle is over a pre-set threshold, and regains energy whenever possible. It was hypothesised that providing torque from the regenerative braking at the time of highest fuel flowrate would have the greatest effect on the overall fuel usage of the vehicle over a cycle.

A CDF of the instantaneous fuel flowrate for each drive cycle was calculated in a similar fashion to the power usage algorithm above, and this CDF is shown in Figure 9. This CDF was used in a similar way to the instantaneous power CDF above and the threshold percentages (to the nearest 5%) are given in Table 2. As with the power consumption controller, the deceleration behaviour was the same as that for the greedy controller. For all drive cycles the fuel usage heuristic gave 0.3-2.1 percentage points improvement in EI_V saving compared to the greedy strategy (see Table 3 and Figure 8).

Time histories of the fuel CDF and power usage heuristic controllers over the UDDS cycle are given in Figure 10. The top graph shows the velocity profile of the UDDS, with a dashed line showing the maximum operational velocity of the PMs (12.7m/s). The middle graph shows the product $a_v.v_v$ for each point in the cycle, with the dashed line showing the

threshold given by the controller. When the $a_v.v_v$ signal is above this line, the PMs are switched on. The lower graph shows the fuel usage during the UDDS cycle, with the dashed line corresponding to the fuel usage threshold. Again, when the fuel usage is above this line, the PMs are switched on.

A magnified version of this plot is shown in Figure 11 in order to highlight the differences between the controllers. This magnified section corresponds to an acceleration from stationary to 11.85m/s. The oscillation in fuel usage (lower graph) between 570s and 575s is caused by gear changes, and closer inspection shows that the threshold has been set just above the fuel flowrate at idle (between 565s and 570s). This means that the regenerative braking system is turned on throughout an acceleration event, rather than being turned off each time the fuel flowrate drops while the time the driver changes gear.

The middle graph shows that the power usage controller only switches on the PMs between 570s and 575s, and then much later at 608-609s. The fuel usage controller, however, turns the regenerative braking system on from 570s to the end of this section. This serves to highlight how different the behaviour of the heuristic controllers can be.

From Table 2 it is clear that there is a large variation in threshold value for each of the two heuristic controllers, and that this depends on the type of the cycle. This in turn means that there is no universal threshold that could be used in all cycles, as even small deviations away from these thresholds would result in degraded performance of the system. It is therefore unlikely that the performance of a heuristic controller would be any better than the greedy controller.

3.2.3 MPC Controller

Model predictive control (MPC) is useful for finding robust and near-optimal control inputs for non-linear or discontinuous systems [33] and is used in hybrid vehicle research [34-39]. It requires a model of the plant to be controlled (in this case the vehicle and the hydraulic regenerative braking system), and is often computationally intensive.

In general MPC tries to optimise the set of control inputs over a future 'prediction horizon':

$$\hat{u} = \{u(k), u(k+1), u(k+2), ..., u(k+H_p)\} \quad (5)$$

where $\hat{u}$ is the set of control inputs, $u()$ is the control input at a given time, k is the current time step, and H_p is the current prediction horizon. Once a control input is chosen, it is fed into the plant for the current time step, the model's time step is incremented, and the process is repeated.

MPC can be used to derive a near-optimal control input for each time step. Normally MPC uses a simplified model of the system to be controlled – one that has been linearised for this purpose. However, as discussed above, this system is non-linear and discontinuous, and so it is difficult to provide a linearised system for use in MPC. Due to these restrictions, the entire vehicle and system is used by the MPC controller.

At each time step, an MPC controller tries all possible control input (on-off) combinations within the prediction horizon, and chooses the combination that minimises the fuel usage. This 'branching' effect is shown in Figure 12 for one axle, where the control horizon is 3 seconds.

The controller then moves forward one time step and repeats the process. If the prediction horizon were infinitely long, it would give a lower bound on the fuel usage for each cycle. However, in order to reduce the computation time at each step, a finite horizon must be used, which in turn reduces the optimality of the resulting control inputs.

For a given horizon of length h seconds, the number of possible combinations of control input is 2^h (as the enable signal is a binary one at 1Hz). The length of the horizon should be longer than a single stop or start event, and ideally encompass several start-stop events in order to capture the interdependency of the control actions for the events. Table 4 shows the number of simulations required at each time step to include the smallest start-stop event (i.e. the shortest time over which a stop-start happens) for each cycle, and the overall number of simulations required. Figure 13 shows how the total simulation time for each cycle increases as the length of the controller preview is increased.

Figure 13 shows that for the controller to consider one of the cycle's stop-starts (a preview of around 15 seconds, see Table 4) the simulation time is in the order of months. If the MPC controller considers several stop-start events at each time step, the simulation time increases exponentially, and could take several years to complete.

An MPC algorithm based on minimising the fuel used was implemented for each of the cycles using a horizon of 10 seconds, which is below the minimum horizon suggested above. The results from this controller are given in Table 3 under the heading 'Ordinary' MPC. These results show that 'ordinary MPC' gives a smaller reduction in EI_v for the legislative drive cycles than the default greedy algorithm. The simulation times for these MPC calculations were all in the range of 12-27 hours, with the UDDS cycle taking the longest.

This simplistic implementation of MPC was improved by so-called 'trimming' of the number of simulations required in three main ways. The first was to always turn the PMs on when a deceleration was demanded, ensuring the capture of as much energy as possible. The next improvements were turning off the PMs when the demanded speed was greater than their maximum operating speed (12.7m/s), or zero. This trimming operation reduced the simulation time of the MPC controller by around 70% (see Table 3), and increased the effectiveness of the algorithm. With this 'trimmed' algorithm, it was possible to increase the horizon time of the controller to 12s and have a similar execution time to that of the 'untrimmed' 10-second horizon controller. The results from the 12-second horizon MPC are included in Table 3 and Figure 14 under the heading 'MPC12 - trimmed'.

A time history, similar to that in Figure 10 is given for MPC and Pattern Search in Figure 15. The top graph shows the UDDS drive cycle, again with a dashed line denoting the 12.7m/s operating limit of the PMs. The lower graph shows the pressure in the high-pressure (HP) accumulator over time for the cycle – the solid line is from the MPC12-trimmed controller, and the dashed line is from the Pattern Search control signal.

A magnified section of these graphs is shown in Figure 16 corresponding to a stop-start manoeuvre from around 10m/s, back up to 12.7m/s. The pressure traces on the lower part of the graph show the differences between the MPC controller and the controller derived from Pattern Search.

The MPC controller can only 'see' 12 seconds ahead (much shorter than the time of this stop-start sequence), so it turns the PMs on at the beginning of this period (990s), using the stored energy. The Pattern Search controller does not use the stored energy to help accelerate the

vehicle between 990 and 995s. Instead, it harvests energy during the stop (1006s-1023s), and uses all of the remaining energy to accelerate the vehicle during the next acceleration phase (1052s-1071s). Over this 90s window, despite starting at approximately the same pressures, the Pattern Search controller has reduced the fuel usage more than the MPC controller by waiting to use the stored energy.

The results in Table 3 show that, for all legislative cycles studied, 'ordinary' MPC provided lower EI_v reductions than 'trimmed' MPC. In addition, the EI_v reductions provided by the 'trimmed' MPC algorithm were very similar to those provided by the greedy algorithm (see Table 3). It is likely that, with a longer prediction horizon, MPC would provide a significantly lower EI_v than greedy. However, as discussed above, a longer prediction horizon results in a significantly longer execution time (see Figure 13).

4 Conclusions

i. A controller network for a hydraulic regenerative braking system was described which includes two layers – a supervisory layer responsible for managing overall demand and a local controller layer for controlling each axle.

ii. Three 'global optimisation' techniques were investigated over four standard drive cycles. The Pattern Search optimiser produced the greatest reduction in EI_v for each cycle, with EI_v reductions of 11-21.9%.

iii. The 'greedy' algorithm is the only control algorithm investigated that can operate in real-time. It provides an EI_v decrease of 9-17%, depending on the drive cycle.

iv. Additional heuristic methods were designed to generate control signals for each of the cycles, and these further reduced the EI_v for some drive cycles. These methods both require 'a-priori 'information about the statistics of the duty cycle. It would be difficult to generate this information accurately in practice. Any non-optimal threshold value would result in reduced performance, making it unlikely that the heuristic controller would be any better than the greedy controller.

v. Two MPC controllers were devised for the system, and provided similar improvements in EI_v to the greedy algorithm, though the improvements depended on the preview horizon time used. These controllers required lengthy computation times and would need to be streamlined significantly to make them suitable for real-time implementation.

5 Funding

This work was supported by the New Zealand Foundation for Research, Science and Technology[2] (Grant number: CAMX0801), the Cambridge Vehicle Dynamics Consortium[3], the Centre for Sustainable Road Freight[4] and EPSRC grant reference: EP/K00915X/1

6 Acknowledgements

The authors would like to thank Poclain Hydraulics for their support, as well as Team MRO for their help with this research. Additionally, none of this research would have been

[2] http://www.msi.govt.nz/

[3] http://www.cvdc.org/

[4] http://www.sustainableroadfreight.com/

possible without the generous technical support of the Cambridge Vehicle Dynamics Consortium whose members at the time of writing were: Camcon, Denby Transport, Firestone Industrial Products, Goodyear Tires, Haldex Brake Products, SDC Trailers, SIMPACK, Mektronika Systems, MIRA, Poclain Hydraulics, Tinsley Bridge, Tridec BV and Volvo Trucks. This research would not have been undertaken without the financial support of the Centre for Sustainable Road Freight, whose members at the time of writing were as follows: Coca-Cola, Freight Transport Association, Laing O'Rourke, Optrak, Tesco, The John Lewis Partnership, Warburtons, and Wincanton.

7 Figures

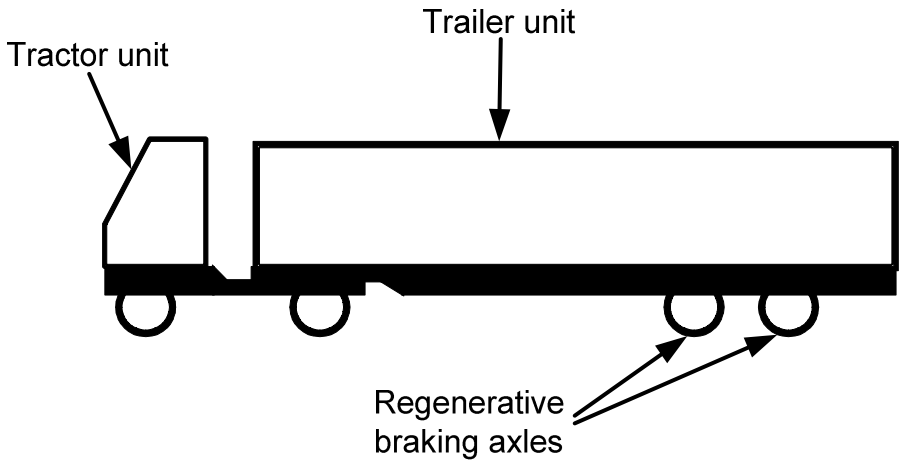

Figure 1 Schematic of tractor-trailer unit showing regenerative braking axles

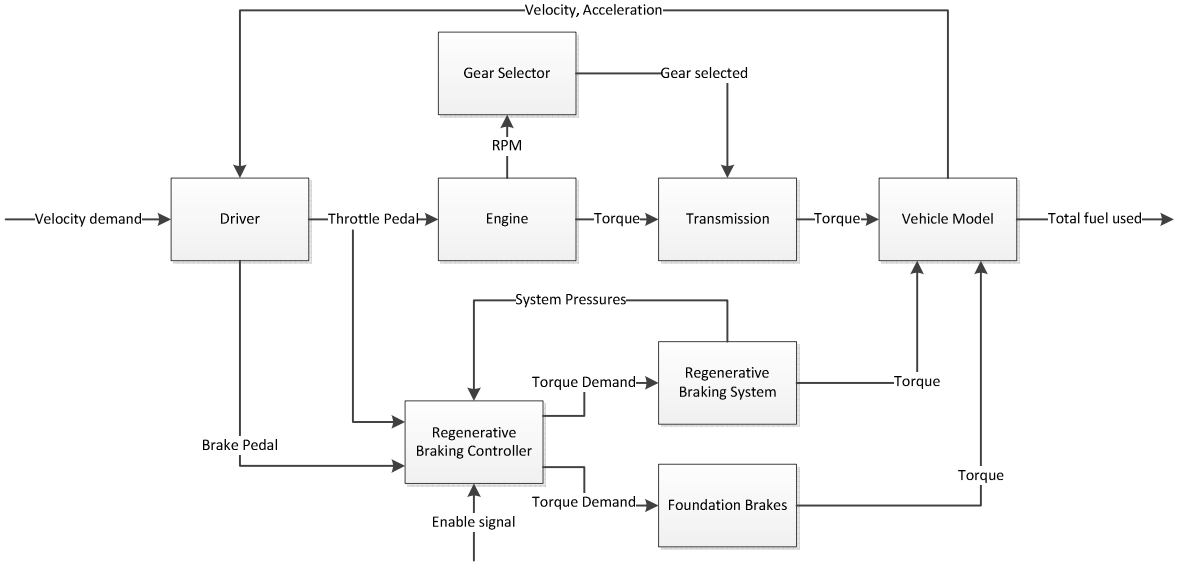

Figure 2 Schematic of vehicle and regenerative braking system model showing system inputs (velocity demand and 1Hz enable signal) and output (fuel usage)

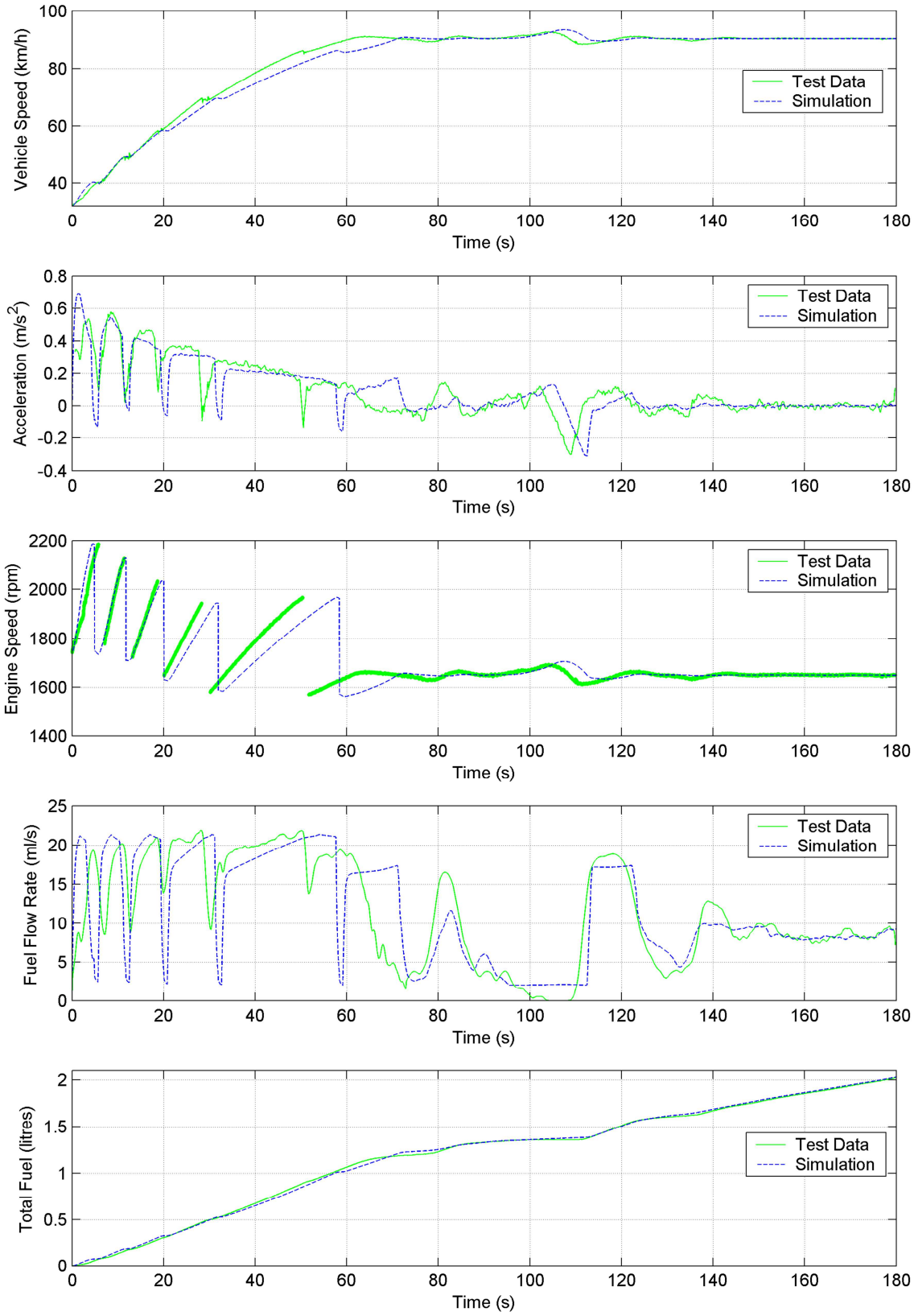

Figure 3 Validation of vehicle model [17]

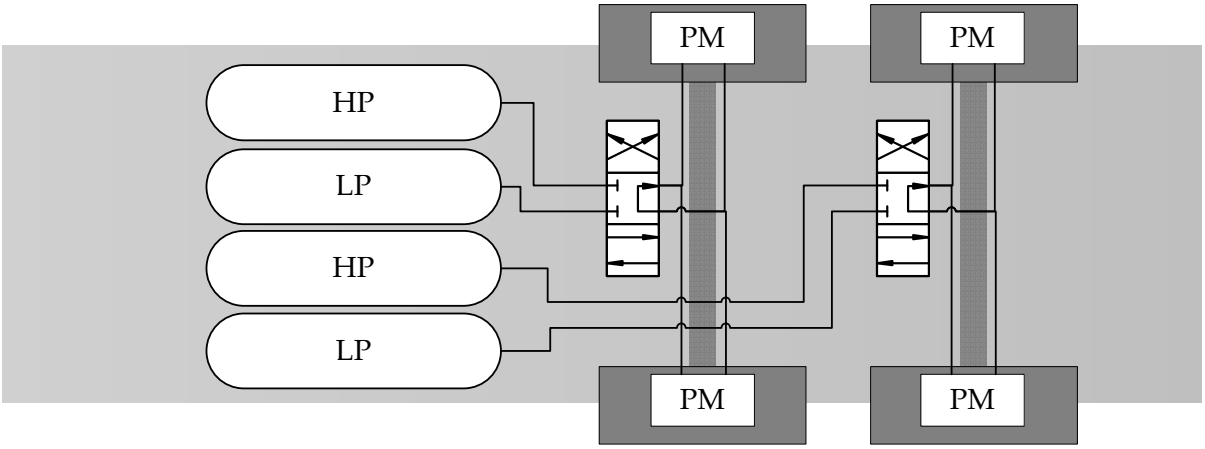

Figure 4 Schematic showing location of hydraulic accumulators on the underbody of the trailer (not to scale)

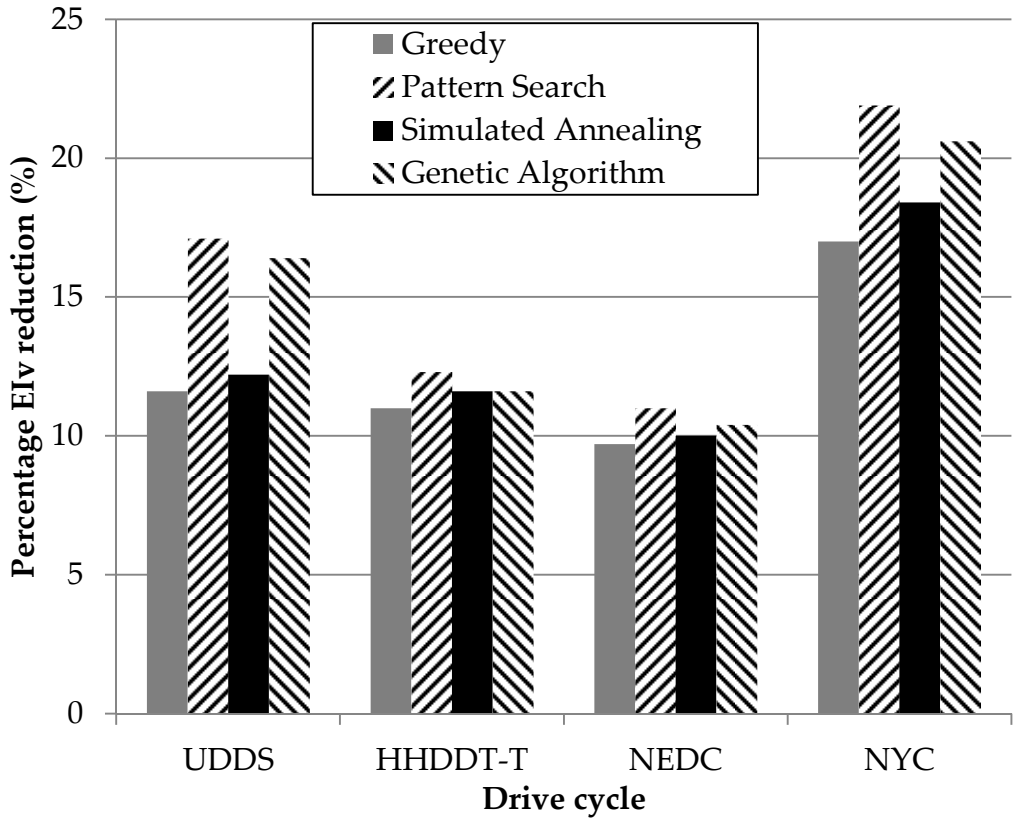

Figure 5 Comparison of optimisers over several drive cycles

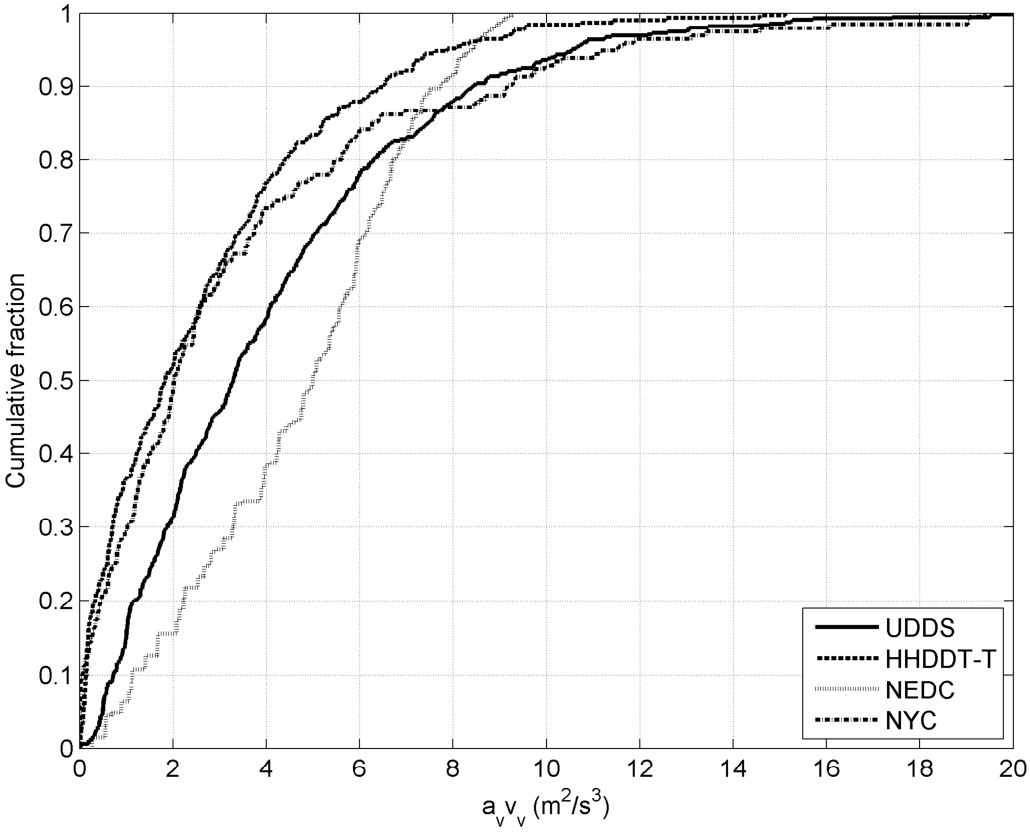

Figure 6 CDF of acceleration multiplied by velocity for the positive acceleration sections of each of the legislative drive cycles

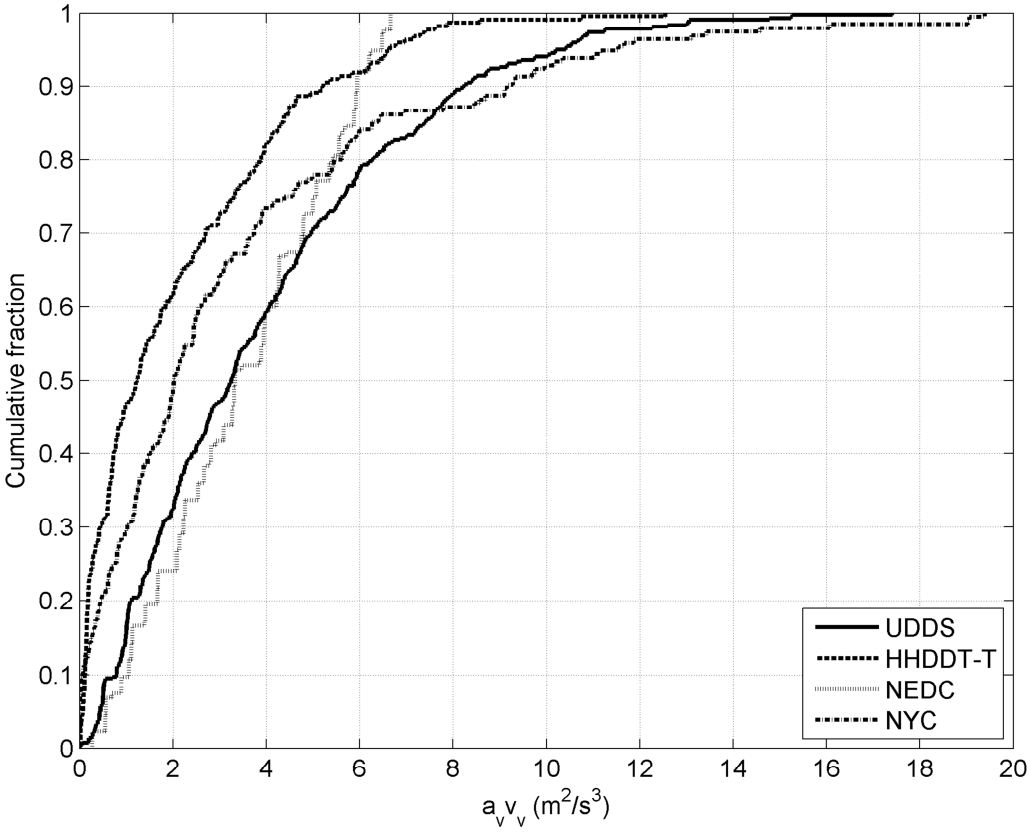

Figure 7 CDF of acceleration times velocity for the positive acceleration and low velocity sections of each of the legislative drive cycles

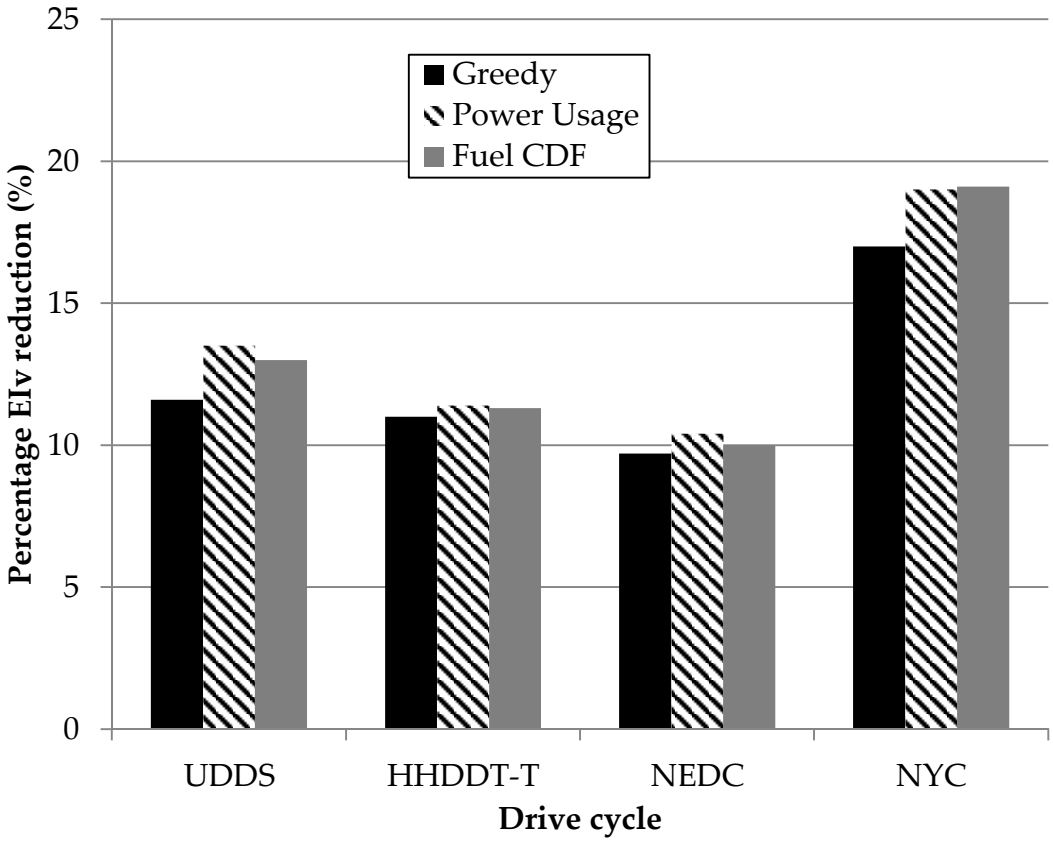

Figure 8 Comparison of heuristic control strategies

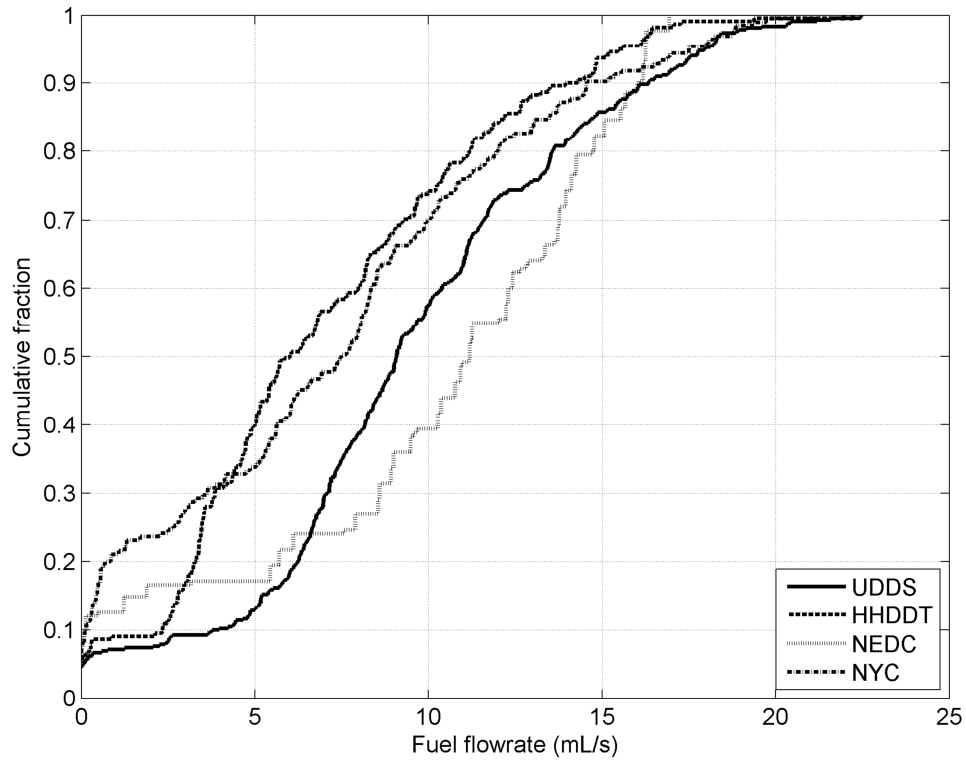

Figure 9 CDF of fuel flowrates for the positive acceleration and low velocity sections of each of the legislative drive cycles

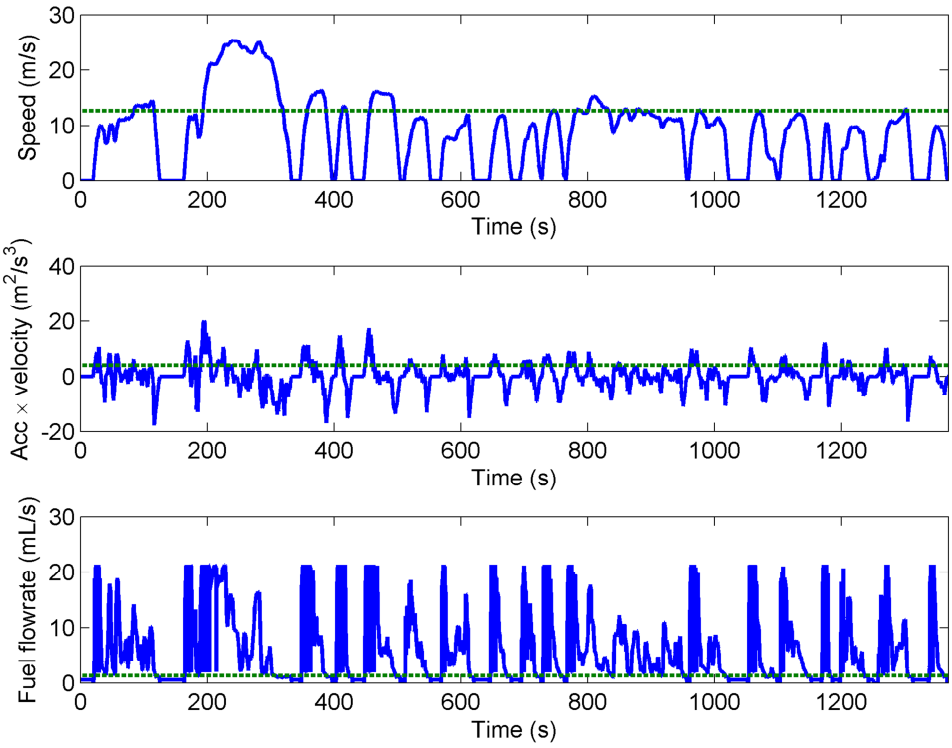

Figure 10 Time histories of heuristic strategies

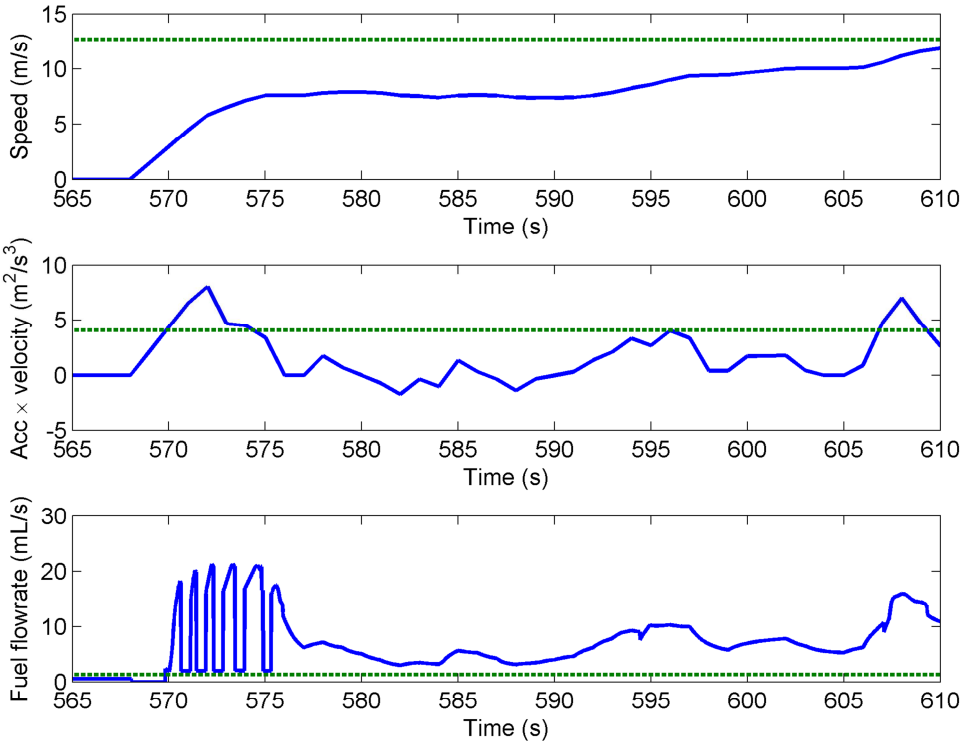

Figure 11 Magnified section of heuristic control strategy time history

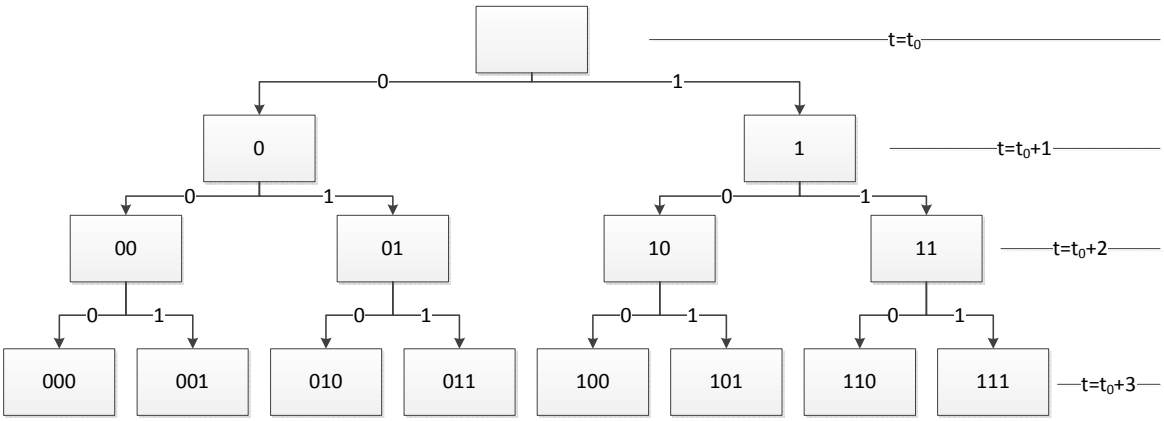

Figure 12 Branching behaviour of MPC control for one axle

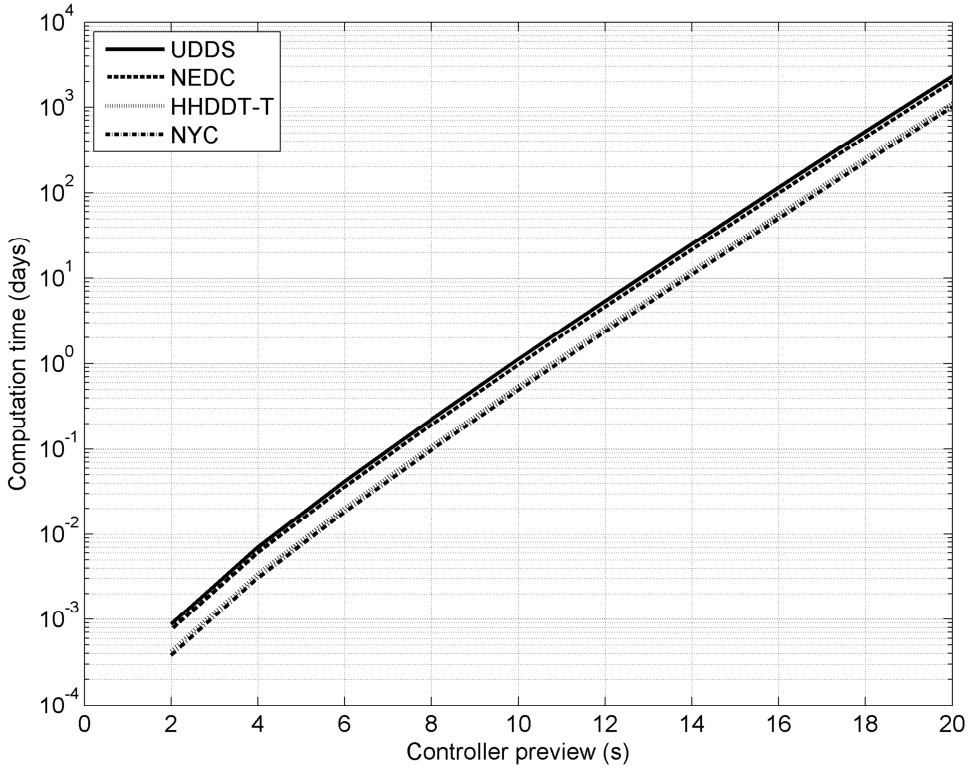

Figure 13 Increase in simulation time as the MPC controller preview length is increased

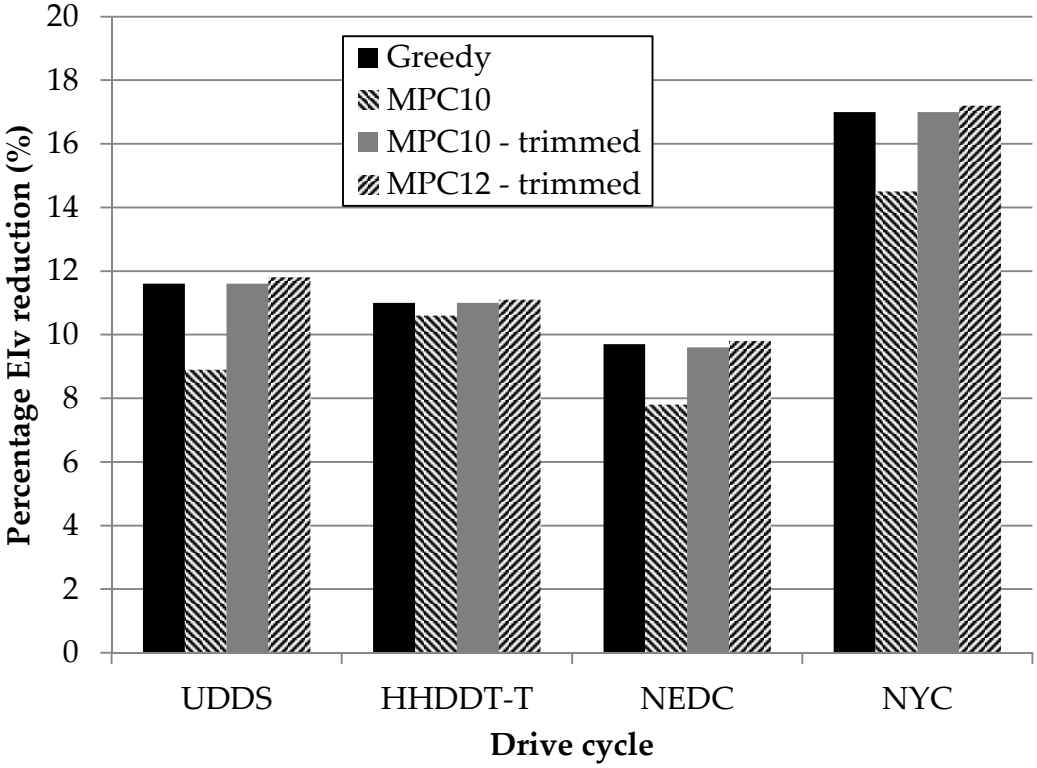

Figure 14 Comparison of MPC results

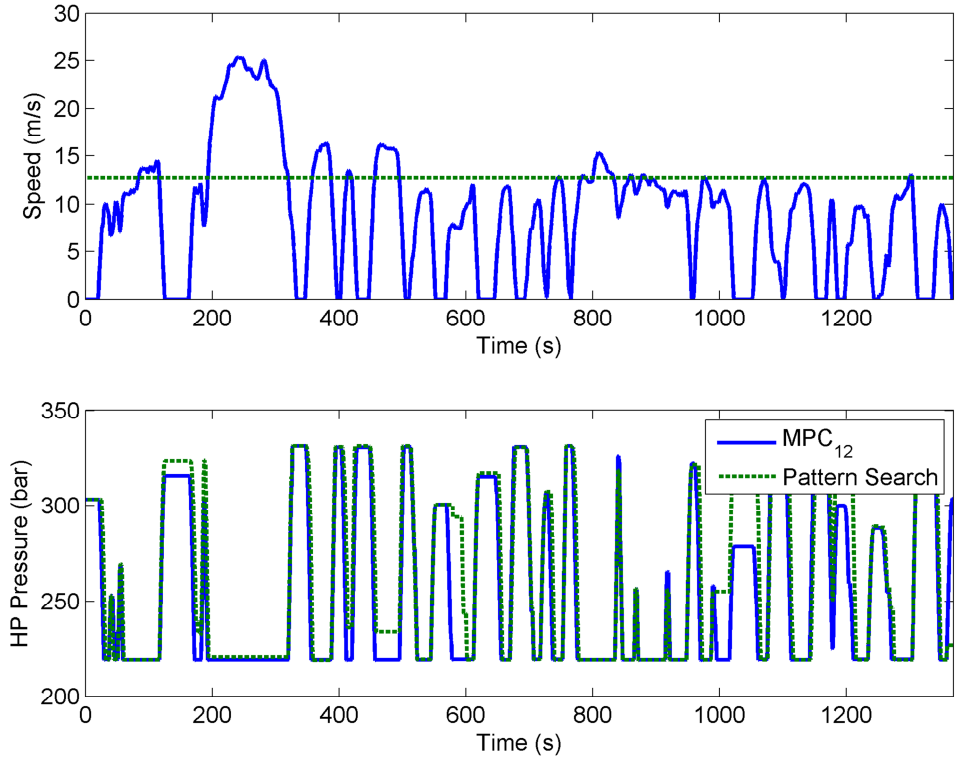

Figure 15 UDDS drive cycle, and time histories of the HP pressure for the MPC_{12} controller and the controller produced by Pattern Search.

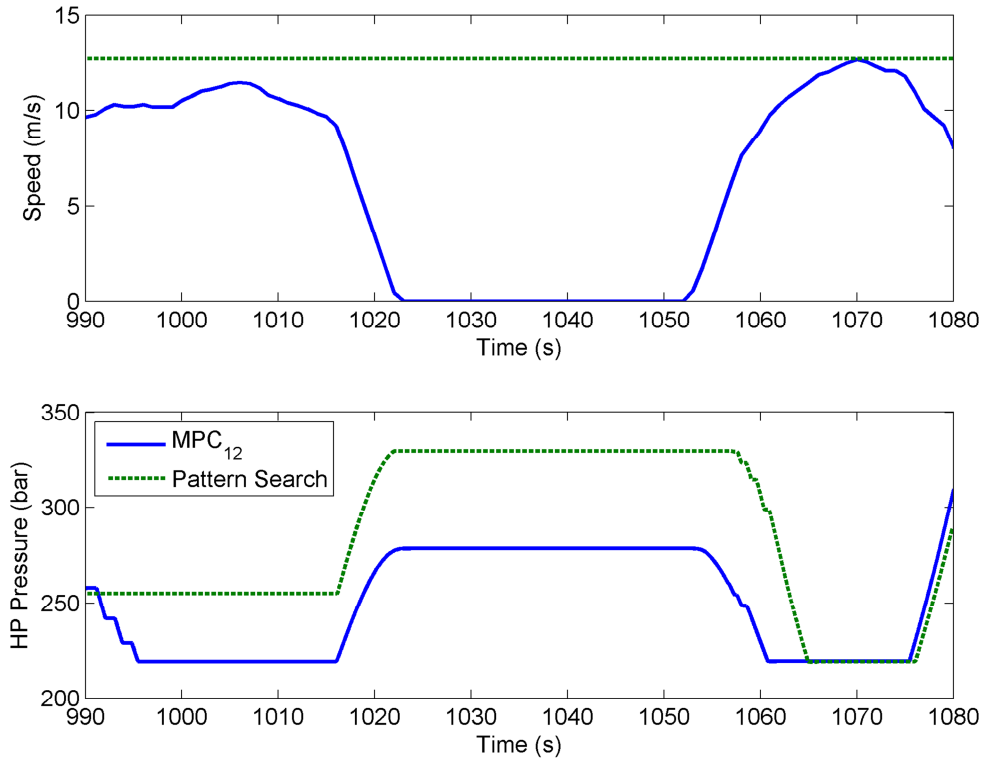

Figure 16 Magnified section of MPC_{12} and Pattern Search time histories

8 Tables

Parameter	Value [Units]
Unladen vehicle mass	19365 [kg]
Maximum trailer payload	84.24 [m^3]
Density of freight	100 [kg/m^3]
Regenerative braking system weight	289 [kg]

Table 1 Key vehicle and model parameters

	Fuel		AV	
	Threshold (%)	Value (mL/s)	Threshold (%)	Value (m^2/s^3)
UDDS	40%	8.2	60%	4.15
HHDDT-T	70%	9.5	40%	0.40
NEDC	60%	12.4	20%	1.41
NY	80%	12.0	60%	2.54

Table 2 Threshold switching levels used for heuristic control strategies

		% EIv Reduction (relative to greedy)			
	Cycle	UDDS	HHDDT-T	NEDC	NYC
	Greedy	11.6	11.0	9.7	17.0
Heuristic	**Power Usage**	13.5 (1.9)	11.4 (0.4)	10.4 (0.7)	19.0 (2.0)
Heuristic	**Fuel CDF**	13.0 (1.4)	11.3 (0.3)	10.0 (0.3)	19.1 (2.1)
Global Optimiser	**Pattern Search**	17.1 (5.5)	12.3 (1.3)	11.0 (1.3)	21.9 (4.9)
Global Optimiser	**Simulated Annealing**	12.2 (0.6)	11.6 (0.6)	10.0 (0.3)	18.4 (1.4)
Global Optimiser	**Genetic Algorithm**	16.4 (4.8)	11.6 (0.6)	10.4 (0.7)	20.6 (3.6)
MPC	**MPC10**	8.9 (-2.7)	10.6 (-0.4)	7.8 (-1.9)	14.5 (-2.5)
MPC	**MPC10 - trimmed**	11.6 (0.0)	11.0 (0.0)	9.6 (-0.1)	17.0 (0.0)
MPC	**MPC12 - trimmed**	11.8 (0.2)	11.1 (0.1)	9.8 (0.1)	17.2 (0.2)

Table 3 EI_v reduction achieved with different control strategies (the best strategy is highlighted).

Cycle	NEDC	UDDS	HHDDT-T	NYC
Smallest start-stop (sec)	17	19	35	12
Length of cycle (sec)	1185	1370	669	599
Number of input combinations/simulations per timestep	131072	524288	3.436E+10	4096
Total number of simulations	155320321	718274561	2.2987E+13	2453505

Table 4 Comparison of input combinations for each drive cycle

9 Nomenclature

ρ – Hydraulic fluid density [kg/m^3]

a_v – Vehicle acceleration [m/s^2]

EI_v – Energy index by volume [kJ/(kg.km)]

$\dot{E}_v$ – Instantaneous vehicle power [W]

h – MPC horizon length [s]

k – Hydraulic loss coefficient [-]

m_v – Vehicle mass [kg]

v_f – Hydraulic fluid velocity [m/s]

v_v – Vehicle velocity [m/s]

10 References and Raw Data

[1] A. M. C. Odhams, R. L. Roebuck, Y. J. Lee, S. W. Hunt, and D. Cebon, "Factors Influencing the Energy Consumption of Road Freight Transport," *Proc IMechE Part C, J Mech Eng Sci,* vol. 224, pp. 1995-2010, 2010.

[2] M. K. Vint and D. B. Gilmore, "Simulation of Transit Bus Regenerative Braking Systems," *Mathematics and Computers in Simulation,* vol. 30, pp. 55-61, 1988.

[3] C.-C. Lin, Z. Filipi, L. Louca, H. Peng, D. Assanis, and J. Stein, "Modelling and control of a medium-duty hybrid electric truck," *International Journal of Heavy Vehicle Systems,* vol. 11, p. 349, 2004.

[4] P. Tona, P. Gautier, and R. Amari, "Modeling and Control of a Mild-Hybrid City Car with a Downsized Turbo-Charged CNG Engine," presented at the 2008 Advanced Vehicle Conference, Kobe, Japan, 2008.

[5] "Hydraulic hybrids boost fuel economy," *Machine Design,* vol. 78, pp. S4-S6, 2006.

[6] W. J. B. Midgley and D. Cebon, "Comparison of Regenerative Braking Technologies for Heavy Goods Vehicles in Urban Environments," *Proceedings of the Institution of Mechanical Engineers, Part D: Journal of Automobile Engineering,* vol. 226, pp. 957-970, 14 March 2012.

[7] W. J. B. Midgley, H. Cathcart, and D. Cebon, "Modelling of hydraulic regenerative braking systems for heavy vehicles," *Proceedings of the Institution of Mechanical Engineers, Part D: Journal of Automobile Engineering,* vol. 227, pp. 1072-1084, July 1, 2013 2013.

[8] C.-C. Lin, J.-M. Kang, J. W. Grizzle, and H. Peng, "Energy management strategy for a parallel hybrid electric truck," in *Proceedings of the 2001 American Control Conference*, Arlington, VA, USA, 2001, pp. 2878-2883.

[9] J. Cao, B. Cao, W. Chen, and P. Xu, "Neural Network Self-adaptive PID Control for Driving and Regenerative Braking of Electric Vehicle," in *2007 IEEE International Conference on Automation and Logistics*, Jinan, China, 2007, pp. 2029-2034.

[10] J. Cao, B. Cao, P. Xu, and Z. Bai, "Regenerative-braking sliding mode control of electric vehicle based on neural network identification," in *IEEE/ASME International Conference on Advanced Intelligent Mechatronics, 2008*, Xian, China, 2008, pp. 1219-1224.

[11] C.-C. Lin, S. Jeon, H. Peng, and J. M. Lee, "Driving Pattern Recognition for Control of Hybrid Electric Trucks," *Vehicle System Dynamics,* vol. 42, pp. 41 - 58, 2004.

[12] C.-C. Lin, H. Peng, S. Jeon, and J. M. Lee, "Control of a Hybrid Electric Truck Based on Driving Pattern Recognition," presented at the Advanced Vehicle Control Conference, Hiroshima, 2002.

[13] C. Dextreit, G. Hannis, K. Burnham, O. C. L. Haas, F. Assadian, and W. Yue, "Power Management Techniques for Hybrid Vehicles," presented at the Eighteenth International Conference on Systems Engineering, Coventry University, 2006.

[14] C.-C. Lin, H. Peng, J. W. Grizzle, and J.-M. Kang, "Power management strategy for a parallel hybrid electric truck," *Control Systems Technology, IEEE Transactions on,* vol. 11, pp. 839-849, 2003.

[15] F. Wang, H. Zhong, X.-J. Mao, L. Yang, and B. Zhuo, "Regenerative braking algorithm for a parallel hybrid electric vehicle with continuously variable transmission," in *IEEE International Conference on Vehicular Electronics and Safety*, Beijing, China, 2007.

[16] W. J. B. Midgley, H. A. Cathcart, and D. Cebon, "Modelling of Hydraulic Regenerative Braking Systems for Heavy Vehicles," *Proceedings of the institution of Mechanical Engineers, Part D: Journal of Automobile Engineering: In Press,* 2012.

[17] S. W. Hunt, A. M. C. Odhams, R. L. Roebuck, and D. Cebon, "Parameter measurement for heavy-vehicle fuel consumption modelling," *Proceedings of the Institution of Mechanical Engineers, Part D: Journal of Automobile Engineering,* vol. 225, pp. 567-589, May 1, 2011 2010.

[18] W. J. B. Midgley, "Hydraulic Regenerative Braking for Urban Delivery Heavy Vehicles," PhD Thesis, Engineering, Cambridge University, 2012.

[19] "CARBONWEIGHT High Pressure Bladder Accumulators," Technical specification - Lightning Hybrids Inc., Colorado2011.
[20] "MF08 - MFE08 Hydrobases - Technical Catalog," Poclain Hydraulics2008.
[21] H. E. Merritt, *Hydraulic Control Systems*: John Wiley & Sons, 1967.
[22] R. P. Kepner, "Hydraulic Power Assist - A Demonstration of Hydraulic Hybrid Vehicle Regenerative Braking in a Road Vehicle Application," *SAE Transactions on Passenger Vehicles,* pp. 826-833, 2002.
[23] A. Charles and J. E. Dennis, Jr., "Analysis of Generalized Pattern Searches," *SIAM J. on Optimization,* vol. 13, pp. 889-903, 2002.
[24] Kirkpatrick, "Optimization by Simulated Annealing," *Science,* vol. 220, p. 671, 1983.
[25] D. E. Goldberg, *Genetic Algorithms in Search, Optimization, and Machine Learning*: Addison-Wesley, 1989.
[26] T. M. Post, P. S. Fancher, and J. E. Bernard, "Torque characteristics of commercial vehicle brakes," *SAE 750210,* 1975.
[27] R. Radlinski, "Development of a truck-tractor pneumatic simulator and optimization of trailer air brake plumbing," Vehicle Research and Test Center, National Highway Traffic Safety Administration, U.S. Dept. of Transport., Memorandum Report CAR-5, April, 1981 1981.
[28] A. C. Collop, D. Cebon, and M. S. A. Hardy, "A visco-elastic approach to rutting in flexible pavements," *ASCE Journal of Transportation Engineering,* vol. 121, pp. 82-93, 1995.
[29] R. Diestel, *Graph Theory*: Springer, 2006.
[30] Z. Filipi and Y. J. Kim, "Hydraulic Hybrid Propulsion for Heavy Vehicles: Combining the Simulation and Engine-In-the-Loop Techniques to Maximize the Fuel Economy and Emission Benefits," *Oil Gas Sci. Technol.,* vol. 65, pp. 155-178, 2010.
[31] L. Wasserman, *All of Nonparametric Statistics*: Springer, 2005.
[32] D. Zwillinger and S. Kokoska, *CRC Standard Probability and Statistics Tables and Formulae*: Taylor & Francis, 1999.
[33] J. B. Rawlings and D. Q. Mayne, *Model predictive control : theory and design*. Madison, Wisconsin: Nob Hill Publishing, 2009.
[34] R. Beck, F. Richert, A. Bollig, D. Abel, S. Saenger, K. Neil, T. Scholt, and K. E. Noreikat, "Model Predictive Control of a Parallel Hybrid Vehicle Drivetrain," in *Decision and Control, 2005 and 2005 European Control Conference. CDC-ECC '05. 44th IEEE Conference on*, 2005, pp. 2670-2675.
[35] A. Zlocki and P. Themann, "Improved energy efficiency by model based predictive ACC in hybrid vehicles based on map data," presented at the AVEC 10, Loughborough, England, 2010.
[36] F. Tavares, R. Johri, and Z. Filipi, "Simulation Study of Advanced Variable Displacement Engine Coupled to Power-Split Hydraulic Hybrid Powertrain," presented at the ASME Internal Combustion Engine Division 2009 Spring Technical Conference, Milwaukee, WI, 2009.
[37] L. Johannesson, M. Asbogard, and B. Egardt, "Assessing the Potential of Predictive Control for Hybrid Vehicle Powertrains Using Stochastic Dynamic Programming," *Intelligent Transportation Systems, IEEE Transactions on,* vol. 8, pp. 71-83, 2007.
[38] H. A. Borhan, A. Vahidi, A. M. Phillips, M. L. Kuang, and I. V. Kolmanovsky, "Predictive energy management of a power-split hybrid electric vehicle," in *American Control Conference, 2009. ACC '09.*, 2009, pp. 3970-3976.
[39] A. Arce, A. J. del Real, and C. Bordons, "MPC for battery/fuel cell hybrid vehicles including fuel cell dynamics and battery performance improvement," *Journal of Process Control,* vol. 19, pp. 1289-1304, 2009.

For access to the raw data used in the production of this paper, please see:
http://www.repository.cam.ac.uk/handle/1810/248831